Pergamon

Int. J. Solids Structures Vol. 32, No. 8/9, pp. 1231–1246, 1995
Copyright © 1995 Elsevier Science Ltd
Printed in Great Britain. All rights reserved
0020-7683/95 $9.50 + .00

0020-7683(94)00145-6

A COMPARATIVE STUDY OF STABILITY OF LAMINATED ANISOTROPIC CYLINDERS UNDER AXIAL COMPRESSION AND TORSION

P. ETITUM† and S.B. DONG
Civil and Environmental Engineering Department, University of California at Los Angeles, CA 90024, U.S.A.

(*Received* 11 *January* 1994; *in revised form* 22 *June* 1994)

Abstract—A parametric study is presented on the accuracy of stability data for axial compression and torsion by classical and first-order shear deformation theories for laminated composite cylinders. Comparisons of the data in the forms of curves of critical stress versus L/a (dimensionless wavelength/radius ratio) are made with those by Biot's theory, which is predicated on three-dimensional elasticity. Two thickness/radius ratios were considered: $H/a = 0.01$ and 0.1, typical of thin and thick shell geometries, respectively. First, a comparison of the data for a homogeneous, isotropic cylinder was given to have a baseline for understanding the role of material anisotropy. Then, a number of regular symmetric and antisymmetric laminates were considered, all laminate profiles based on one material system only, that of $E_L/E_T = 25$. The data for thin geometries ($H/a \geq 0.01$) showed that classical theory for laminated composite shells can be trusted to give accurate results over a reasonably wide range of L/a. For the thick shell geometry, there were regions of relatively good agreement and regions where classical and first-order shear deformation theories were not appropriate.

INTRODUCTION

The characteristically low transverse stiffnesses in laminated composite materials render them more susceptible to transverse shear and normal deformations. Classical plate and shell theory disregards all such deformations and its range of validity for laminated composite structures suffers in comparison to that for homogeneous, isotropic structures. Refined theories account for these effects and currently many such theories are available, each accommodating some level of transverse effects. By and large, the effectiveness and range of validity of all theories for laminated composite plates and shells have not been explored thoroughly with respect to the role of the transverse mechanical properties.

Herein, this type of investigation is reported on stability calculations for laminated composite circular cylindrical cylinders. A parametric study is presented, which compares the bifurcation loads of such cylinders under axial compression and torsion by (1) classical theory, (2) first-order shear deformation theory, and (3) three-dimensional elasticity based on Biot's incremental theory (1965). The parameters of interest include the thickness/radius ratio, number of plies comprising the laminate profile, and orientation of the elastic axes of the constituent materials. Since three-dimensional theory is free of all kinematic hypotheses underlying shell theories and may be regarded as exact, some quantitative sense of the ranges of validity of classical and first-order shear deformation theories can be gained from this study. The stability of such tubes by Biot's theory was studied in a companion paper by Dong and Etitum (1994).

Many stability analyses of laminated shells based on classical theory have been reported in the literature. Comprehensive review papers by Ambartsumian (1974), Tennyson (1975) and Simitses (1986) chronicle the state-of-the-art. With respect to the circular cylinder, Simitses and Han (1991a, b) summarized the relevant literature and presented an extensive parametric study on buckling under axial compression, lateral pressure and hydrostatic pressure. Lou and Yaniv (1991) analysed the stability of composite cylindrical shells under axial compression and bending and presented data comparing the results based on the

†Currently a Director of Vibro(Thai) Ltd., Bangkok, Thailand.

theories of Love and Donnell. The numerical (and graphical) data in these references provide insight into the roles of the length/radius (L/a) ratio, radius/thickness (a/H) ratio and stacking sequence. While refined theories for laminated cylindrical shells have appeared in the literature, applications to stability are limited. Simitses and Anastasiadis (1991) conducted a parametric study on axial compression buckling of laminated cylindrical shells, based on first-order shear deformation and higher-order theories. An important finding from their investigation is that transverse shear deformations constituted the major correction beyond classical theory for cylinders that are moderately thick (their study was limited to $a/H \geqslant 15$), confirming that shear is more important than transverse normal strain in a priority of refinements. However, the accuracy of the stability data and/or the range of validity of the various shell theories were not addressed. To clarify understanding of these issues, shell theory results should be compared with that using three-dimensional elasticity.

The laminated cylindrical shell equations for classical and first-order shell theories used herein are those due to Dong *et al.* (1962) and Dong and Chun (1992), respectively. In the next section, the equations for first-order shear deformation theory are summarized. In the subsequent section, equations for classical theory are obtained as a special case by dismissing transverse shear deformations. The terms related to the initial stress state entering into the stability calculations are those belonging to Flügge's theory (1962).

Buckled shapes that are periodic in the axial and circumferential directions are substituted into the governing equations of equilibrium to formulate algebraic eigenvalue problems. Periodic solution forms for laminated orthotropic or cross-ply cylinders pertain to simply supported boundary conditions at the two ends of a cylinder. For angle-ply cylinders, there is no meaningful physical analogue of simple supports. Nevertheless, these results will be compared with three-dimensional elasticity data using the same solution forms, thus the data are commensurable. The results appear in the form of plots of critical stress (load) versus the normalized buckled wavelength.

It is recognized that initial imperfections in cylindrical shells play an important role in buckling analyses, as evidenced by the voluminous literature as cited by Hutchinson and Koiter (1970) for homogeneous, isotropic cylinders and Simitses (1986) for laminated composite cylinders. Imperfections are not taken up here because the parameters chosen to be studied will by themselves occupy considerable attention.

FIRST-ORDER SHEAR DEFORMATION THEORY

First-order shear deformation theory represents the initial correction of classical theory in terms of a priority of corrections. Figure 1 shows a circular cylinder whose mean radius is denoted by a. Adopt cylindrical coordinates (x, θ, r) with (x, θ) spanning the adopted reference surface of the laminated cylinder. Let (u, v, w) and (β_x, β_θ) denote the displacement components and bending rotations with respect to the adopted reference. The kinetic variables are the five force and three moment resultants $(N_{xx}, N_{\theta\theta}, N_{x\theta}, Q_x, Q_\theta, M_{xx}, M_{\theta\theta}, M_{x\theta})$ defined by

$$(N_{xx}, N_{\theta\theta}, N_{x\theta}, Q_x, Q_\theta) = \int_h (\sigma_{xx}, \sigma_{\theta\theta}, \sigma_{x\theta}, \sigma_{xr}, \sigma_{\theta r})\, \mathrm{d}r \tag{1}$$

$$(M_{xx}, M_{\theta\theta}, M_{x\theta}) = \int_h (\sigma_{xx}, \sigma_{\theta\theta}, \sigma_{x\theta}) r\, \mathrm{d}r. \tag{2}$$

The initial stress or prebuckled state is composed of given stress resultants $(\bar{N}_{xx}, \bar{N}_{\theta\theta}, \bar{N}_{x\theta})$, which herein is assumed to be uniform and in equilibrium.

The strain–displacement relations of first-order shear deformation theory for circular cylindrical shells are

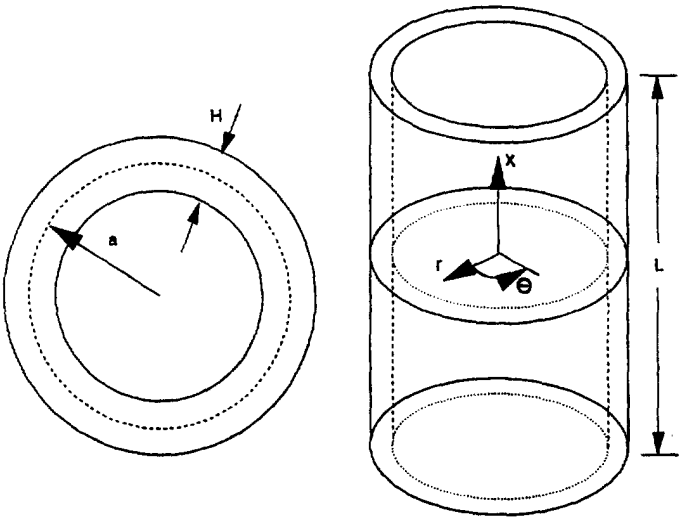

Notes: "a" denotes the mean radius of the cylindrical shell.

0° Ply Angle is parallel to the x-axis.

Fig. 1. Diagram of cylindrical shell coordinate system.

$$\varepsilon_{xx} = u_{,x}, \quad \varepsilon_{\theta\theta} = \frac{1}{a}(v_{,\theta} + w), \quad \gamma_{x\theta} = v_{,x} + \frac{1}{a}u_{,\theta} \tag{3}$$

$$\kappa_{xx} = \beta_{x,x}, \quad \kappa_{\theta\theta} = \frac{1}{a}\beta_{\theta,\theta}, \quad \kappa_{x\theta} = \beta_{\theta,x} + \frac{1}{a}\beta_{x,\theta} \tag{4}$$

$$\gamma_{xr} = w_{,x} + \beta_x, \quad \gamma_{\theta r} = \frac{1}{a}(w_{,\theta} - v) + \beta_\theta, \tag{5}$$

where $(\varepsilon_{xx}, \varepsilon_{\theta\theta}, \gamma_{x\theta})$ and $(\kappa_{xx}, \kappa_{\theta\theta}, \kappa_{x\theta})$ are the reference surface strains and changes of curvatures, respectively, and $(\gamma_{xr}, \gamma_{\theta r})$ are the transverse shear angles.

The inplane stress and moment resultants are related to the deformation measures by

$$\begin{bmatrix} \mathbf{N} \\ \mathbf{M} \end{bmatrix} = \begin{bmatrix} \mathbf{A} & \mathbf{B} \\ \mathbf{B} & \mathbf{D} \end{bmatrix} \begin{bmatrix} \boldsymbol{\varepsilon} \\ \boldsymbol{\kappa} \end{bmatrix} \tag{6}$$

where $\mathbf{N}^T = [N_{xx}, N_{\theta\theta}, N_{x\theta}]$, $\mathbf{M}^T = [M_{xx}, M_{\theta\theta}, M_{x\theta}]$, $\boldsymbol{\varepsilon}^T = [\varepsilon_{xx}, \varepsilon_{\theta\theta}, \gamma_{x\theta}]$, and $\boldsymbol{\kappa}^T = [\kappa_{xx}, \kappa_{\theta\theta}, \kappa_{x\theta}]$ and $\mathbf{A}, \mathbf{B}, \mathbf{D}$ in eqn (6) denote the 3×3 submatrices of inplane, coupling and bending stiffnesses defined by

$$(A_{ij}, B_{ij}, D_{ij}) = \int_h Q_{ij}^{(k)}(1, r, r^2)\, dr \quad (i, j = 1, 2, 6) \tag{7}$$

with Q_{ij}s as the reduced elastic moduli of the kth layer. In addition to constitutive relation (6), there is a shear constitutive relation for a first-order shear deformation theory of the form

$$\begin{bmatrix} Q_x \\ Q_\theta \end{bmatrix} = \begin{bmatrix} \Gamma_{55} & \Gamma_{45} \\ \Gamma_{45} & \Gamma_{44} \end{bmatrix} \begin{bmatrix} \gamma_{xr} \\ \gamma_{\theta r} \end{bmatrix} \tag{8}$$

where $(\Gamma_{55}, \Gamma_{44}, \Gamma_{45})$ are the transverse shear rigidities which may be defined in terms of the integrals of transverse shear moduli $(Q_{55}^{(k)}, Q_{44}^{(k)}, Q_{45}^{(k)})$ over the laminate profile and shear correction factors $(k_{55}^2, k_{44}^2, k_{45}^2)$ as

$$\Gamma_{55} = k_{55}^2 A_{55}, \quad \Gamma_{44} = k_{44}^2 A_{44}, \quad \Gamma_{45} = k_{45}^2 A_{45} \tag{9}$$

$$(A_{55}, A_{44}, A_{45}) = \int_h (Q_{55}^{(k)}, Q_{44}^{(k)}, Q_{45}^{(k)})\, \mathrm{d}r. \tag{10}$$

The values of the shear correction factors are discussed in the paper by Dong and Chun (1992).

The stress and moment resultants satisfy the following five equilibrium equations which are expressed with respect to the prebuckled equilibrium configuration:

$$aN_{xx,x} + N_{x\theta,\theta} - a\bar{N}_{xx}u_{,xx} - 2\bar{N}_{x\theta}u_{,x\theta} - \bar{N}_{\theta\theta}\left(\frac{1}{a}u_{,\theta\theta} + w_{,x}\right) = 0 \tag{11}$$

$$aN_{x\theta,x} + N_{\theta\theta,\theta} + Q_\theta - a\bar{N}_{xx}v_{,xx} - 2\bar{N}_{x\theta}(v_{,x\theta} - w_{,x}) - \frac{1}{a}\bar{N}_{\theta\theta}(v_{,\theta\theta} - w_{,\theta}) = 0 \tag{12}$$

$$aQ_{x,x} + Q_{\theta,\theta} - N_{\theta\theta} + a\bar{N}_{xx}w_{,xx} + 2\bar{N}_{x\theta}(v_{,x} + w_{,x\theta}) - \bar{N}_{\theta\theta}\left(u_{,x} - \frac{1}{a}v_{,\theta} - \frac{1}{a}w_{,\theta\theta}\right) = 0 \tag{13}$$

$$aM_{xx,x} + M_{x\theta,\theta} - aQ_x = 0 \tag{14}$$

$$aM_{x\theta,x} + M_{\theta\theta,\theta} - aQ_\theta = 0. \tag{15}$$

Displacement equations of equilibrium are obtained by substituting strain–displacement relations (3)–(5) and constitutive relations (6) and (8) in eqns (11)–(15). The results expressed in abbreviated matrix notation are

$$[L_s]\{\mathbf{u}_s\} = (\bar{N}_{xx}[L_{sg1}] + \bar{N}_{x\theta}[L_{sg2}] + \bar{N}_{\theta\theta}[L_{sg3}])\{\mathbf{u}_s\} \tag{16}$$

where

$$\{\mathbf{u}_s\}^{\mathrm{T}} = [u, v, w, \beta_x, \beta_\theta] \tag{17}$$

and $[L_s]$, $[L_{sg1}]$, $[L_{sg2}]$ and $[L_{sg3}]$ are 5×5 matrices of differential operators which are defined in Appendix A.

CLASSICAL THEORY

Classical theory rests upon ignoring transverse shear deformations. Setting $\gamma_{xr} = \gamma_{x\theta} = 0$ in eqn (5) gives the bending rotations as

$$\beta_x = -w_{,x}, \quad \beta_\theta = -\frac{1}{a}(w_{,\theta} - v). \tag{18}$$

Therefore, in classical theory there are only three kinematic variables, namely the reference

surface displacements u, v, w. With the absence of shear deformation, shear constitutive equation (8) has no role and only eqn (6) relating the extensional/bending deformations to their corresponding forces and moments is relevant. The shear resultants can only be determined by equilibrium considerations.

The strain–displacement relations for classical theory are

$$\varepsilon_{xx} = u_{,x}, \quad \varepsilon_{\theta\theta} = \frac{1}{a}(v_{,\theta} + w), \quad \gamma_{x\theta} = v_{,x} + \frac{1}{a}u_{,\theta} \tag{19}$$

$$\kappa_{xx} = -w_{,xx}, \quad \kappa_{\theta\theta} = -\frac{1}{a^2}(w_{,\theta\theta} - v_{,\theta}), \quad \kappa_{x\theta} = -\frac{1}{a}(2w_{,x\theta} - v_{,x}). \tag{20}$$

Note that eqn (19) is identical to eqn (3), but eqn (20) is obtained from eqn (4) by means of eqn (18). Since there is no transverse shear constitutive relation, it is necessary to eliminate the shear resultants from equilibrium equations (11)–(14) to give

$$aN_{xx,x} + N_{x\theta,\theta} - a\bar{N}_{xx}u_{,xx} - 2\bar{N}_{x\theta}u_{,x\theta} - \bar{N}_{\theta\theta}\left(\frac{1}{a}u_{,\theta\theta} + w_{,x}\right) = 0 \tag{21}$$

$$aN_{x\theta,x} + N_{\theta\theta,\theta} + M_{x\theta,x} + \frac{1}{a}M_{\theta\theta,\theta} - a\bar{N}_{xx}v_{,xx} - 2\bar{N}_{x\theta}(v_{,x\theta} - w_{,x}) - \frac{1}{a}\bar{N}_{\theta\theta}(v_{,\theta\theta} - w_{,\theta}) = 0 \tag{22}$$

$$aM_{xx,xx} + 2M_{x\theta,x\theta} + \frac{1}{a}M_{\theta\theta,\theta\theta} - N_{\theta\theta} + a\bar{N}_{xx}w_{,xx} + 2\bar{N}_{x\theta}(w_{,x\theta} + v_{,x}) - \bar{N}_{\theta\theta}\left(u_{,x} - \frac{1}{a}v_{,\theta} - \frac{1}{a}w_{,\theta\theta}\right) = 0. \tag{23}$$

Displacement equations of equilibrium are obtained by substituting eqns (19), (20) and (6) into eqns (21)–(23). In abbreviated matrix notation, they take the form

$$[L_c]\{\mathbf{u}_c\} = (\bar{N}_{xx}[L_{cg1}] + \bar{N}_{x\theta}[L_{cg2}] + \bar{N}_{\theta\theta}[L_{cg3}])\{\mathbf{u}_c\} \tag{24}$$

where $\{\mathbf{u}_c\}$ is the vector with three displacement components, i.e.

$$\{\mathbf{u}_c\}^{\mathrm{T}} = [u, v, w], \tag{25}$$

and $[L_c]$, $[L_{cg1}]$, $[L_{cg2}]$ and $[L_{cg3}]$ are 3×3 matrices of differential operators which are defined in Appendix B.

STABILITY ANALYSIS—THE EIGENVALUE/EIGENVECTOR PROBLEMS

The buckled mode shapes are taken as periodic functions in the axial and circumferential directions. The solution forms for classical and first-order deformation theories are

$$\{\mathbf{u}_c\} = \begin{bmatrix} U \\ V \\ W \end{bmatrix} \exp\{\mathrm{i}(kx+n\theta)\} = \{U_{co}\} \exp\{\mathrm{i}(kx+n\theta)\} \tag{26}$$

$$\{\mathbf{u}_s\} = \begin{bmatrix} U \\ V \\ W \\ B_x \\ B_\theta \end{bmatrix} \exp\{\mathrm{i}(kx+n\theta)\} = \{U_{so}\} \exp\{\mathrm{i}(kx+n\theta)\}. \tag{27}$$

Substituting these forms into eqns (21)–(23) and (11)–(15) gives, respectively,

$$[K_c(k,n)]\{U_{co}\} = \Lambda\,(R_1[K_{cg1}(k,n)] + R_2[K_{cg2}(k,n)] + R_3[K_{cg3}(k,n)])\{U_{co}\} \tag{28}$$

$$[K_s(k,n)]\{U_{so}\} = \Lambda\,(R_1[K_{sg1}(k,n)] + R_2[K_{sg2}(k,n)] + R_3[K_{sg3}(k,n)])\{U_{so}\} \tag{29}$$

where the elements of all stiffness and geometric stiffness matrices in eqns (28) and (29) are given in the two Appendices, and R_1, R_2, R_3 are defined as

$$R_1 = \bar{N}_{xx}/\Lambda, \quad R_2 = \bar{N}_{\theta\theta}/\Lambda, \quad R_3 = \bar{N}_{x\theta}/\Lambda \tag{30}$$

and Λ is the eigenvalue parameter representing the ratio of the critical stress state to the given initial stress state. An examination of the forms of all matrices in eqns (28) and (29), as given in the two Appendices, shows that they are hermitian. Therefore, real eigenvalues are contained in these algebraic eigensystems. The eigenvectors, which may be complex, represent the relative modal amplitudes of the periodic buckled shapes.

HOMOGENEOUS, ISOTROPIC CYLINDER

In this section, the critical stresses for a homogeneous, isotropic cylinder under uniform axial compression and torsion by the three approaches are compared. The stability data appear as curves of critical dimensionless axial and shear stresses, $N_{xx\,\mathrm{cr}}/EH$ and $N_{x\theta\,\mathrm{cr}}/EH$, versus normalized wavelength L/a. On these curves, the circumferential mode numbers associated with the critical stresses are also indicated. By assessing the accuracy of the stability data for a homogeneous, isotropic cylinder, a meaningful baseline is established for observing the role of material anisotropy in laminated composite cylinders. In this study, Poisson's ratio ν was taken as 0.3. Two thickness/radius ratios were considered: $H/a = 0.01$ and 0.1 representing thin and thick shell geometries, respectively. The values of the transverse rigidities and shear correction factors in the first-order shear deformation theory are $\Gamma_{55} = \Gamma_{44} = 0.3846$, $\Gamma_{45} = 0$ and $k_{55}^2 = k_{44}^2 = 5/6$ and $k_{45}^2 = 0$.

The axial compression data appear in Fig. 2. For $H/a = 0.01$, excellent agreement between the three approaches is seen over the entire L/a range. For $H/a = 0.1$, the correlation is reasonably good for $L/a > 0.5$. It is pointed out that for large L/a, the asymptotic character of the critical stress for both thick and thin shell geometries abides by Euler's column formula, i.e. it is proportional to $(L/a)^2$. This behavior is reckoned from the slope of the critical stress curves, which on a log–log basis, gives the exponent 2.

The torsion data comparison is shown in Fig. 3. The initial torsion state used in Biot's theory is a linearly varying shear stress through the thickness with its force resultant equivalent to the value of $\bar{N}_{x\theta}$ that is used in the shell theories. The agreement between the three approaches suffers in comparison with respect to the axial compression data. For both H/a cases, the shell theories underpredict the critical stress. In the large L/a range, there is a uniform difference between the elasticity results and those of the shell theories. One important comment regarding the behavior in the large L/a range needs to be made.

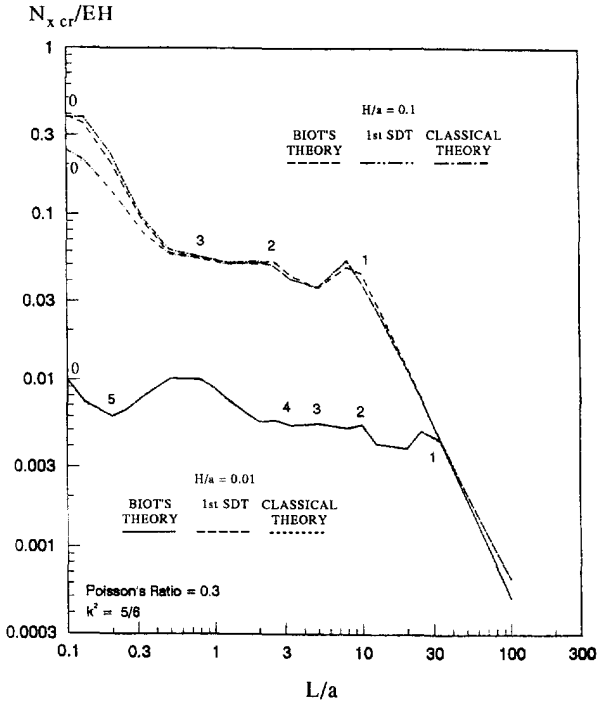

Fig. 2. Axial compression stability of a homogeneous, isotropic cylinder.

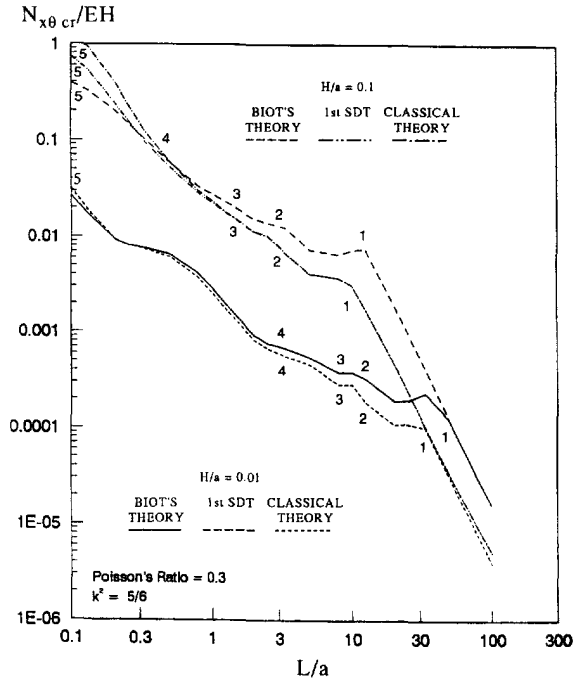

Fig. 3. Torsional stability of a homogeneous, isotropic cylinder.

The calculations show the critical shear stress to be associated with circumferential mode $n = 1$. It is well documented that this modal behavior is precluded if some kinematic restraints are present at the ends of the cylinder [see Flügge (1962) or Brush and Almroth (1975) for examples]. For this mode to eventuate, the two ends must rotate in opposite senses so that the nodal lines are helices on the cylinder's surface. Nevertheless, the comparative data are meaningful to the extent that commensurate conditions were used in all

Table 1. Transverse shear rigidities for laminated composite cylinders

Laminate profile	Number of layers	Γ_{55}	Γ_{44}	Γ_{45}
Cross-ply	2	0.353020	0.353020	0.0
	3	0.394147	0.322227	0.0
$\pm 45^\circ$	2	0.353030	0.353020	0.0
Angle-ply	3	0.358187	0.358187	0.035460
$\pm 30^\circ$	2	0.355000	0.357300	0.0
Angle-ply	3	0.376106	0.339263	0.007012

three approaches. For laminated composite cylinders discussed in the subsequent section, this observation also applies.

In both cases of axial compression and torsion, the data for $H/a = 0.1$ in the range $L/a < 1$ show a complete lack of correlation. In this region, the displacement distributions based on Biot's theory reveal the presence of considerable transverse normal and surface shear deformations, which are obviously beyond the realm of the shell theories. Plots illustrating this behavior in ($\pm 45^\circ$) laminated composite cylinders appear in Figs 7 and 8, so that no diagrams are given for the homogeneous, isotropic cylinder.

LAMINATED COMPOSITE CYLINDERS

Comparisons of stability data for laminated composite cylinders under axial compression and torsion data are presented in this section. In this study, only one material system was considered, whose properties are

$$\frac{E_L}{E_T} = 25, \quad \frac{G_{LT}}{E_T} = 0.5, \quad \frac{G_{TT}}{E_T} = 0.4, \quad \nu_{LT} = 0.25, \quad \nu_{TT} = 0.25. \tag{31}$$

The laminate profiles based on this material to be studied include regular symmetric (three layers) and antisymmetric (two layers) cross-ply and angle-ply ($\pm 45^\circ$ and $\pm 30^\circ$) laminates. In Table 1 are given the transverse shear rigidities Γ_{55}, Γ_{44}, Γ_{45} used in the first-order shear deformation theory. These shear rigidities were determined using a methodology given by Dong and Chun (1992). Again, only two thickness/radius ratios were considered, i.e. $H/a = 0.01$ and 0.1, where H represents the total thickness of the laminate profile.

Dimensionless axial stress curves $N_{xx\,cr}/E_T H$ versus L/a are shown in Figs 4–6. It is remarked that the initial state used in the Biot's theory calculations involve a uniform axial

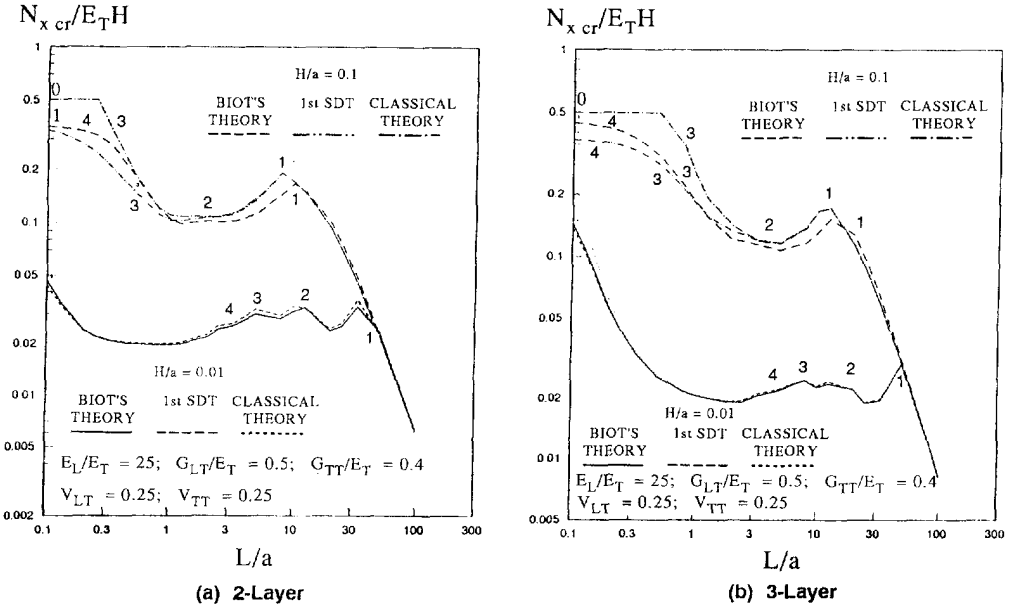

Fig. 4. Axial compression stability of regular symmetric and antisymmetric cross-ply cylinders.

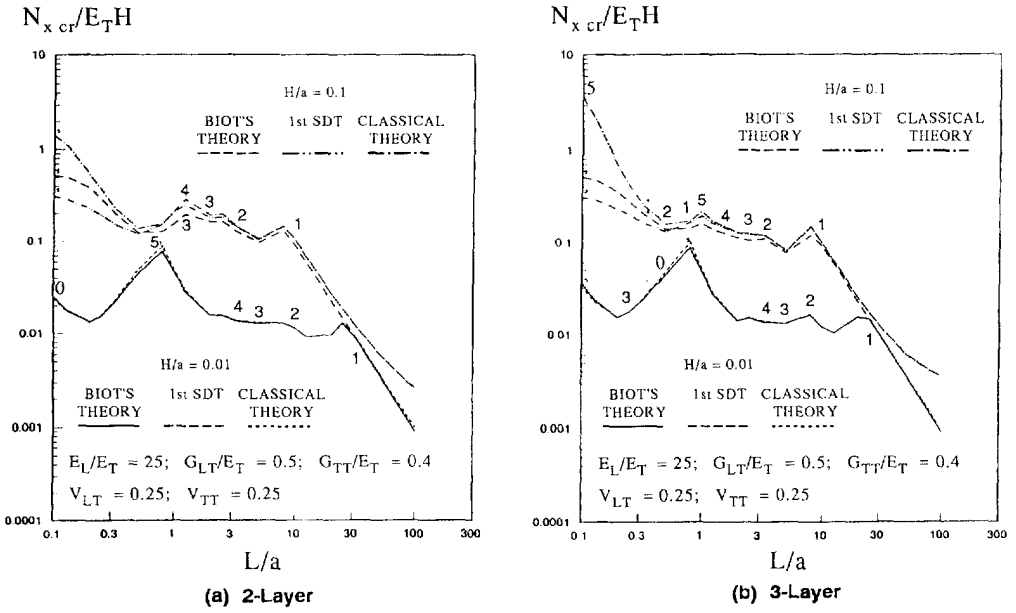

Fig. 5. Axial compression stability of regular symmetric and antisymmetric ($\pm 45°$) angle-ply cylinders.

strain over the total cross-section. For both angle-ply cylinders, this strain state translates to a uniform axial stress state over the entire cross-section. For the cross-ply laminates, the axial stresses in the (0°) and (90°) ply orientations are proportional to E_L and E_T, respectively, and the integrals of the stress over the cross-section are equated to the axial force $\bar{N}_{xx}$, the value used in the shell theories. For $H/a = 0.01$, the data from all three approaches agree remarkably well over the entire L/a range. For $H/a = 0.1$, the correlation suffers by comparison to that for $H/a = 0.01$. For discussion purposes in the thick geometry case, three distinct L/a regions may be identified: (1) $L/a < 1$; (2) $1 < L/a < 15$; (3) $L/a > 15$. In the second range, i.e. $1 < L/a < 15$, the data for all laminates agree reasonably well, although not to the same degree as the homogeneous, isotropic cylinder. For $L/a > 15$, the shell results for the angle-ply cylinders, both ($\pm 45°$) and ($\pm 30°$) cases (Figs 5 and 6)), converge onto curves that are different to those by Biot's theory, and the difference in the critical axial stress grows with L/a. This behavior is absent in the cross-ply cylinders in Fig. 4. For $L/a < 1$, there is no correlation between the three approaches. Moreover, the classical theory data appear to be closer to the elasticity results than the first-order shear deformation theory data, which is fortuitous. In Figs 7 and 8, the displacement plots over the laminate thickness (by elasticity theory) for the two and three layer ($\pm 45°$) laminate profiles for $L/a = 0.1$ indicate the presence of considerable normal and surface shear deformations. Neither effect is modeled by the kinematics of the shell theories.

Torsion data showing dimensionless shear stress $N_{x\theta\,cr}/E_TH$ in terms of L/a are shown in Figs 9–11. Since the shear moduli in each laminate profile is homogeneous over the thickness, the initial shear stress state in Biot's theory follows the elementary torsion formula, i.e. linearly varying stress in the radial direction. A study of the curves in Figs 9–11 shows that the correlation is qualitatively similar to that for the homogeneous, isotropic cylinder except with slightly more scatter. It was noted that for the homogeneous, isotropic cylinder, the elasticity data exhibit a uniform difference to that by the shell theories in the large L/a range, and this feature is in evidence again for the laminated composite cylinders. In this range, there is a difference in the results for $H/a = 0.1$ and 0.01 in the angle-ply cylinders, as each geometric ratio case converges onto its own curve independent of the shell theory. In other words, the geometrical parameter H/a appears to have a larger role in the large L/a range. Moreover, this feature is absent in the data for cross-ply cylinders, indicating ply orientation as another influence. However, these observations must be tempered by noting that the data pertain to circumferential mode number $n = 1$; recall

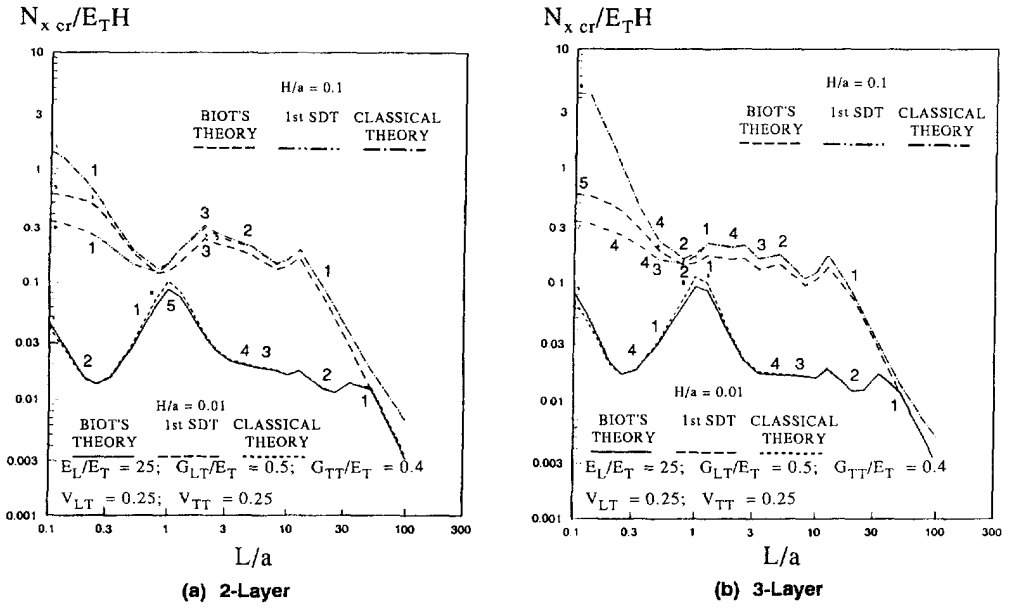

Fig. 6. Axial compression stability of regular symmetric and antisymmetric ($\pm 30°$) angle-ply cylinders.

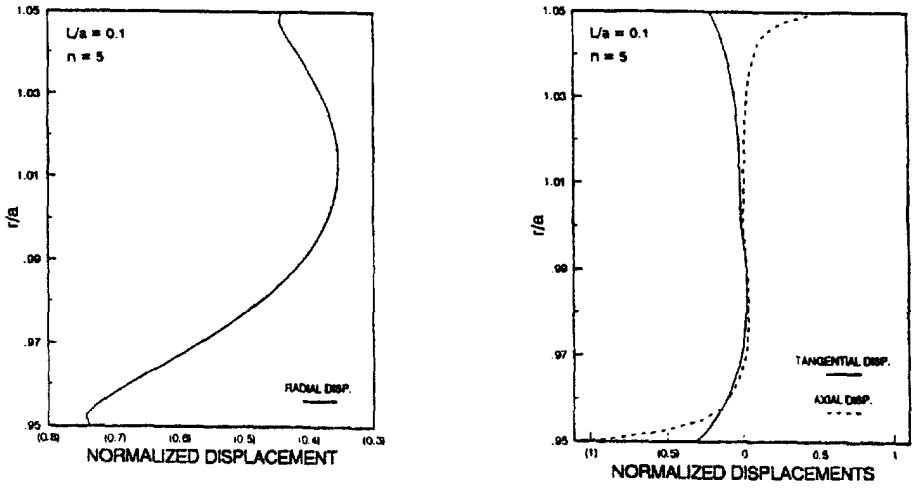

Fig. 7. Displacement eigenvectors for axial compression stability of a regular antisymmetric (45°) two layer angle-ply cylinder.

that realistic end restraints may alter the conclusion regarding this difference between cross-ply and angle-ply cylinders. In the short L/a range, there is essentially no correlation of the data for $H/a = 0.1$. For the torsion loading condition, the first-order shear deformation theory data lie closer to that by elasticity, which again is fortuitous. Displacement distributions by Biot's theory (not given here as they are similar to the axial compression case as presented in Figs 7 and 8) show considerable transverse normal and surface shear deformations.

Stability data and displacement plots for symmetric and antisymmetric profiles, with the number of layers ranging up to six and seven, may be found in the doctoral dissertation of Etitum (1993). In general, the behavioral trends by the two shell theories and elasticity are approximately the same as those presented herein.

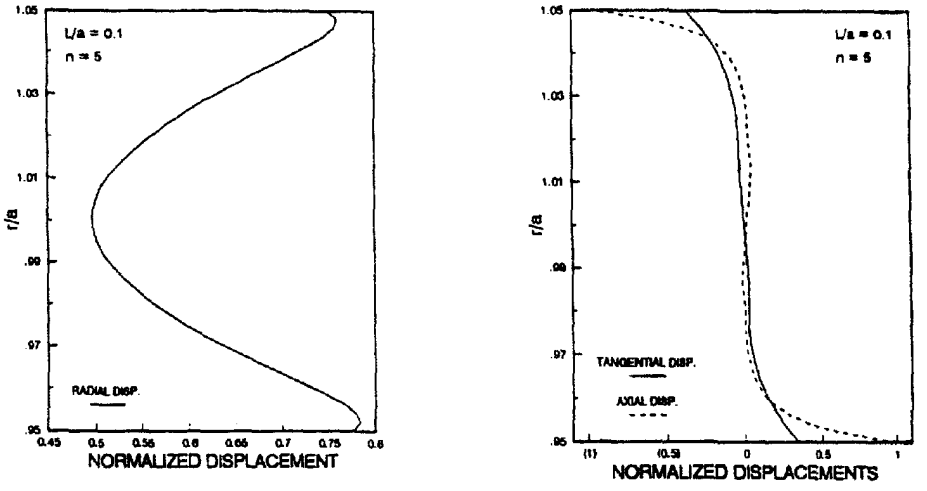

Fig. 8. Displacement eigenvectors for axial compression stability of a regular symmetric (45°) three layer angle-ply cylinder.

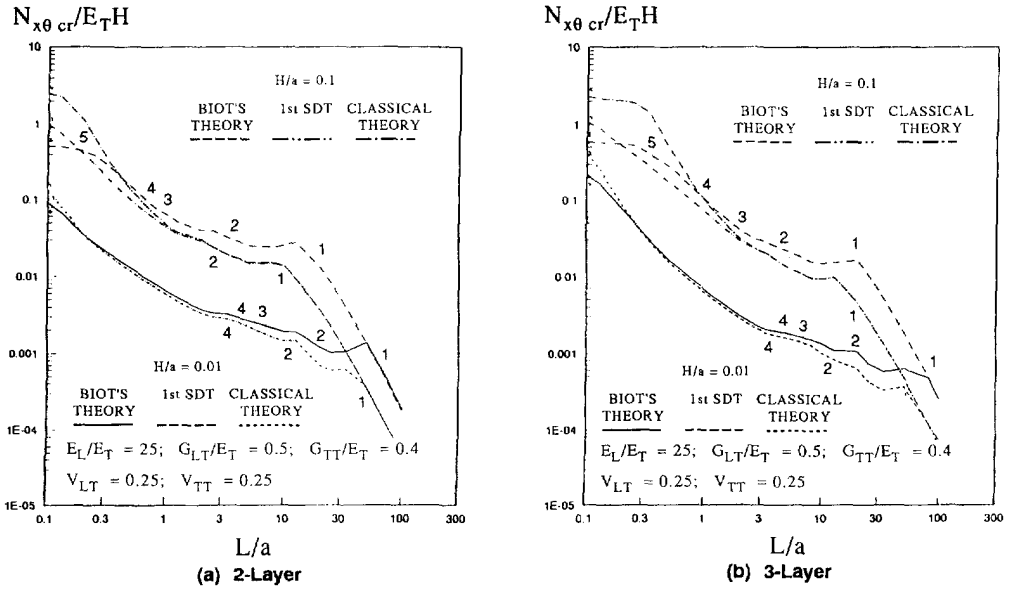

Fig. 9. Torsional stability of regular symmetric and antisymmetric cross-ply cylinders.

CONCLUDING REMARKS

A parametric study was presented on the accuracy of stability data for axial compression and torsion for laminated, anisotropic cylinders by classical and first-order shear deformation theories. The comparison was made with results by Biot's theory, which is predicated on the hypotheses underlying three-dimensional elasticity and taken as the bases herein. The study considered a number of regular symmetric and antisymmetric laminates based on one material system only, where $E_L/E_T = 25$. Two thickness/radius ratios, $H/a = 0.01$ and 0.1, were considered, where these two values were chosen to be representative of thin and thick shell geometries.

This study showed that for thin geometries ($H/a \geqslant 0.01$), classical theory for laminated composite shells can be trusted to give accurate results in the range $0.5 < L/a < 30$. In the same L/a range, the comparisons for $H/a = 0.1$ exhibited reasonable correlation, but the laminated anisotropic data were qualitatively poorer than the homogeneous, isotropic data.

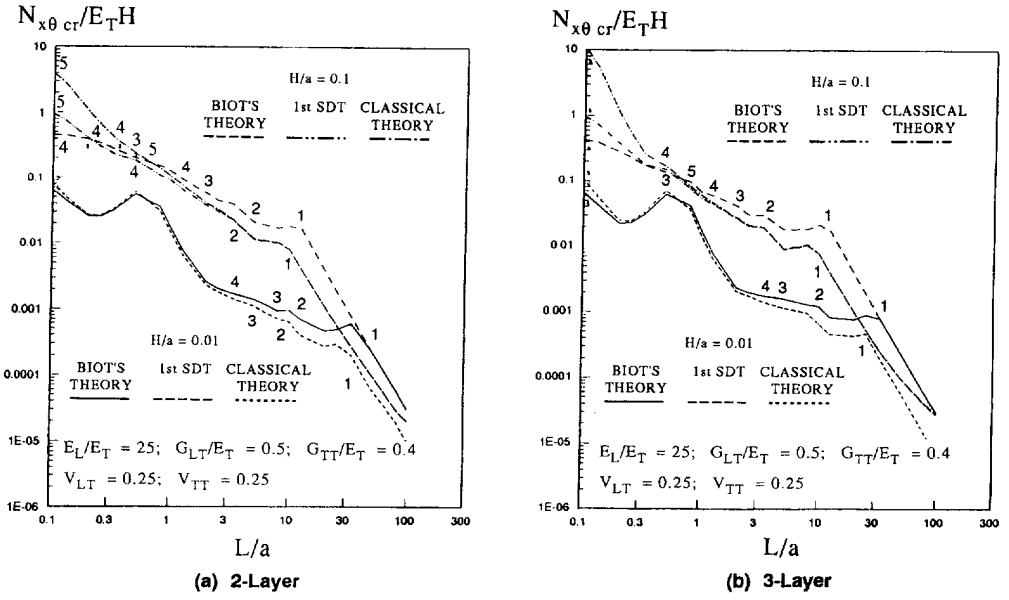

Fig. 10. Torsional stability of regular symmetric and antisymmetric ($\pm 45°$) angle-ply cylinders.

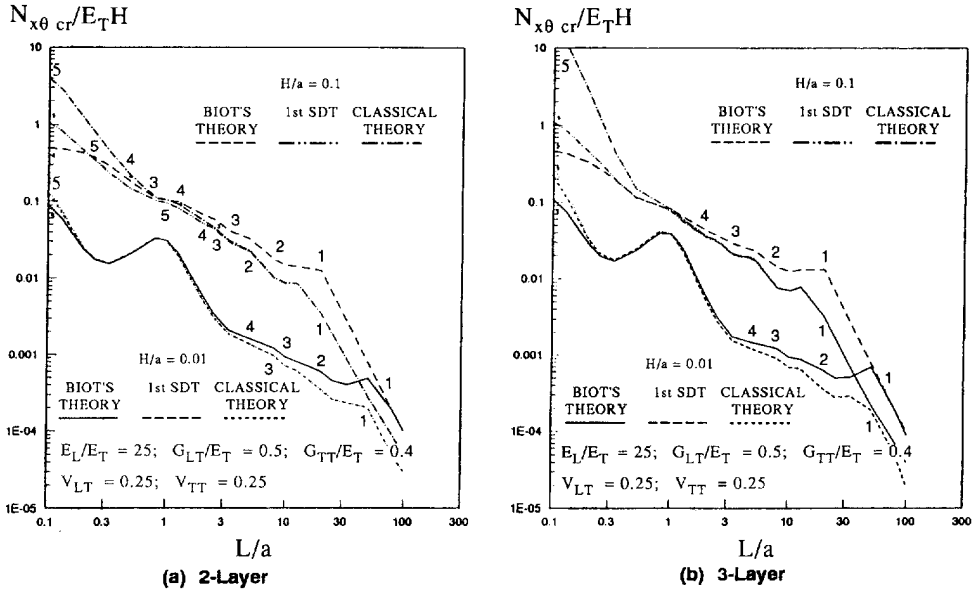

Fig. 11. Torsional stability of regular symmetric and antisymmetric ($\pm 30°$) angle-ply cylinders.

In the long L/a range, there were differences between the results by the shell theories and elasticity for both axial compression and torsion loading conditions, which suggests shortcomings in the kinematic fields of the shell theories. In the short L/a range for the thick shell geometry case, a complete lack of correlation was witnessed. Displacement profiles by elasticity theory indicate the presence of transverse normal and surface shear deformations in this L/a region. It is conjectured that by using a higher-order theory accommodating both normal and shear deformations, this gap between a technical theory approach and elasticity might be lessened.

REFERENCES

Ambartsumian, S. A. (1974). *General Theory of Anisotropic Shells*. Nauka, Moscow.
Biot, M. A. (1965). *Mechanics of Incremental Deformations*. Wiley, New York.
Brush, D. O. and Almroth, B. O. (1975). *Buckling of Bars, Plates and Shells*. McGraw-Hill, New York.

Dong, S. B. and Chun, C. K. (1992). Shear constitutive relations for laminated anisotropic shells and plates. Part I—methodology. *J. Appl. Mech.* **59**(2), 372–379.
Dong, S. B. and Etitum, P. (1994). Three-dimensional stability analysis of laminated anisotropic cylinders. *Int. J. Solids Structures* **31,** SS262.
Dong, S. B., Pister, K. S. and Taylor, R. L. (1962). On the theory of laminated anisotropic shells and plates. *J. Aerospace Sci.* **29**(8), 969–975.
Etitum, P. (1993). Stability analysis of laminated composite cylinders. Ph.D. Dissertation, Department of Civil and Environmental Engineering, University of California, Los Angeles, CA.
Flügge, W. (1962). *Stresses in Shells.* Springer-Verlag, Berlin.
Hutchinson, J. W. and Koiter, W. T. (1970). Postbuckling theory. *Appl. Mech. Rev.* **23**(12),1353–1366.
Lou, K. A. and Yaniv, G. (1991). Buckling of circular cylindrical composite shells under axial compression and bending loads. *J. Composite Mater.* **25,** 162–187.
Simitses, G. J. (1986). Buckling and postbuckling of imperfect cylindrical shells: a review. *Appl. Mech. Rev.* **39**(10), 1517–1524.
Simitses, G. J. and Anastasiadis, J. S. (1991). Buckling of axially-loaded moderately-thick cylindrical laminated shells. *Composites Engng* **1**(6), 375–391.
Simitses, G. J. and Han, B. (1991a). Analysis of laminated cylindrical shells subjected to destabilizing loads. Part I: Theory and solution procedure. *Composite Struct.* **19,** 167–181.
Simitses, G. J. and Han, B. (1991b). Analysis of laminated cylindrical shells subjected to destabilizing loads. Part II: numerical results. *Composite Struct.* **19,** 183–205.
Tennyson, R. C. (1975). Buckling of laminated composite cylinders: a review. *Composites* **6**(1), 17–24.
17–24.

APPENDIX A

The differential operators, stiffness, geometrical stiffness and mass matrices for the first-order shear deformation theory are defined in this Appendix.

$[L_s]$ *operator*

$$L_{s11}() = A_{11}()_{,xx} + \frac{2A_{16}}{a}()_{,x\theta} + \frac{A_{66}}{a^2}()_{,\theta\theta}$$

$$L_{s12}() = L_{s21}() = A_{16}()_{,xx} + \frac{A_{12}+A_{66}}{a}()_{,x\theta} + \frac{A_{26}}{a^2}()_{,\theta\theta}$$

$$L_{s13}() = L_{s31}() = \frac{1}{a}\left(A_{12}()_{,x} + \frac{A_{26}}{a}()_{,\theta}\right)$$

$$L_{s14}() = L_{s41}() = B_{11}()_{,xx} + \frac{2B_{16}}{a}()_{,x\theta} + \frac{B_{66}}{a^2}()_{,\theta\theta}$$

$$L_{s15}() = L_{s51}() = B_{16}()_{,xx} + \frac{B_{12}+B_{66}}{a}()_{,x\theta} + \frac{B_{26}}{a^2}()_{,\theta\theta}$$

$$L_{s22}() = A_{66}()_{,xx} + \frac{2A_{26}}{a}()_{,x\theta} + \frac{A_{22}}{a^2}()_{,\theta\theta} - \frac{\Gamma_{44}}{a^2}()$$

$$L_{s23}() = L_{s32}() = \frac{1}{a}\left((A_{26}+\Gamma_{45})()_{,x} + \frac{A_{22}+\Gamma_{44}}{a}()_{,\theta}\right)$$

$$L_{s24}() = L_{s42}() = B_{16}()_{,xx} + \frac{B_{12}+B_{66}}{a}()_{,x\theta} + \frac{B_{26}}{a^2}()_{,\theta\theta} + \frac{\Gamma_{45}}{a}()$$

$$L_{s25}() = L_{s52}() = B_{66}()_{,xx} + \frac{2B_{26}}{a}()_{,x\theta} + \frac{B_{22}}{a^2}()_{,\theta\theta} + \frac{\Gamma_{44}}{a}()$$

$$L_{s33}() = \frac{A_{22}}{a^2}() - \Gamma_{55}()_{,xx} - \frac{2\Gamma_{45}}{a}()_{,x\theta} - \frac{\Gamma_{44}}{a^2}()_{,\theta\theta}$$

$$L_{s34}() = L_{s43}() = \left(\frac{B_{12}}{a} - \Gamma_{55}\right)()_{,x} + \frac{1}{a}\left(\frac{B_{26}}{a} - \Gamma_{45}\right)()_{,\theta}$$

$$L_{s35}() = L_{s53}() = \left(\frac{B_{26}}{a} - \Gamma_{45}\right)()_{,x} + \frac{1}{a}\left(\frac{B_{22}}{a} - \Gamma_{44}\right)()_{,\theta}$$

$$L_{s44}() = D_{11}()_{,xx} + \frac{2D_{16}}{a}()_{,x\theta} + \frac{D_{66}}{a^2}()_{,\theta\theta} - \Gamma_{55}()$$

$$L_{s45}() = L_{s54}() = D_{16}()_{,xx} + \frac{D_{12}+D_{66}}{a}()_{,x\theta} + \frac{D_{26}}{a^2}()_{,\theta\theta} - \Gamma_{45}()$$

$$L_{s55}() = D_{66}()_{,xx} + \frac{2D_{26}}{a}()_{,x\theta} + \frac{D_{22}}{a^2}()_{,\theta\theta} - \Gamma_{44}().$$

$[L_{sg1}]$. *operator*

$$L_{sg1-11}() = L_{sg1-22}() = -L_{sg1-33}() = ()_{,xx}, \quad \text{all other } L_{sg1-ij}\text{s are zero.}$$

$[L_{sg2}]$ *operator*

$$L_{sg2-11}() = L_{sg2-22}() = L_{sg2-33}() = \frac{2}{a}()_{,x\theta}$$

$$L_{sg2-32}() = -L_{sg2-23}() = \frac{2}{a}()_{,x}, \quad \text{all other } L_{sg2-ij}\text{s are zero.}$$

$[L_{sg3}]$ *operator*

$$L_{sg3-11}() = L_{sg3-22}() = -L_{sg3-33}() = \frac{1}{a^2}()_{,\theta\theta}$$

$$L_{sg3-32}() = -L_{sg3-23}() = \frac{1}{a^2}()_{,\theta}$$

$$L_{sg3-13}() = -L_{sg3-31}() = \frac{1}{a}()_{,x}, \quad \text{all other } L_{sg3-ij}\text{s are zero.}$$

The stiffness matrix $[k_s(k, n)]$ in eqn (29) is complex, i.e.

$$[k_s(k, n)] = [k_{sr}(k, n)] + \mathrm{i}[k_{si}(k, n)],$$

whose nonzero real and imaginary components are

$$k_{sr11} = A_{11}k^2 + 2A_{16}k\bar{n} + A_{66}\bar{n}^2$$

$$k_{sr12} = k_{sr21} = A_{16}k^2 + (A_{12} + A_{66})k\bar{n} + A_{26}\bar{n}^2$$

$$k_{sr14} = k_{sr41} = B_{11}k^2 + 2B_{16}k\bar{n} + B_{66}\bar{n}^2$$

$$k_{sr15} = k_{sr51} = B_{16}k^2 + (B_{12} + B_{66})k\bar{n} + B_{26}\bar{n}^2$$

$$k_{sr22} = A_{66}k^2 + 2A_{26}k\bar{n} + A_{22}\bar{n}^2 + \frac{\Gamma_{44}}{a^2}$$

$$k_{sr24} = k_{sr42} = B_{16}k^2 + (B_{12} + B_{66})k\bar{n} + B_{26}\bar{n}^2 - \frac{\Gamma_{45}}{a}$$

$$k_{sr25} = k_{sr52} = B_{66}k^2 + B_{26}k\bar{n} + B_{22}\bar{n}^2 - \frac{\Gamma_{44}}{a}$$

$$k_{sr33} = \frac{A_{22}}{a^2} + \Gamma_{55}k^2 + 2\Gamma_{45}k\bar{n} + \Gamma_{44}\bar{n}^2$$

$$k_{sr44} = D_{11}k^2 + 2D_{16}k\bar{n} + D_{66}\bar{n}^2 + \Gamma_{55}$$

$$k_{sr45} = k_{sr54} = D_{16}k^2 + (D_{12} + D_{66})k\bar{n} + D_{26}\bar{n}^2 + \Gamma_{45}$$

$$k_{sr55} = D_{66}k^2 + 2D_{26}k\bar{n} + D_{22}\bar{n}^2 + \Gamma_{44}$$

$$k_{si13} = -k_{si31} = -\frac{1}{a}(A_{12}k + A_{26}\bar{n})$$

$$k_{si23} = -k_{si32} = -\frac{1}{a}((A_{26} + \Gamma_{45})k + (A_{22} + \Gamma_{44})\bar{n})$$

$$k_{si34} = -k_{si43} = \left(\frac{B_{12}}{a} - \Gamma_{55}\right)k + \left(\frac{B_{26}}{a} - \Gamma_{45}\right)\bar{n}$$

$$k_{si}35 = -k_{si}53 = \left(\frac{B_{26}}{a} - \Gamma_{45}\right)k + \left(\frac{B_{22}}{a} - \Gamma_{44}\right)\bar{n}.$$

The geometric stiffness matrices in eqn (29) have the forms

$$[k_{sg1}(k)] = [k_{sg1r}(k)]$$

$$[k_{sg2}(k, n)] = [k_{sg2r}(k, n)] + \mathrm{i}\,[k_{sg2i}(k, n)]$$

$$[k_{sg3}(k,n)] = [k_{sg3r}(k,n)] + i\,[k_{sg3i}(k,n)]$$

whose nonzero real and imaginary components are

$$k_{sg1r-11} = k_{sg1r-22} = -k_{sg1r-33} = k^2.$$

There are no imaginary components in $[K_{sg1}]$.

$$k_{sg2r-11} = k_{sg2r-22} = k_{sg2r-33} = 2k\bar{n}$$

$$k_{sg2i-23} = -k_{sg2i-32} = \frac{2k}{a}$$

$$k_{sg3r-11} = k_{sg3r-22} = -k_{sg3r-33} = \bar{n}^2$$

$$k_{sg3i-31} = -k_{sg3i-13} = \frac{k}{a}$$

$$k_{sg3i-23} = -k_{sg3i-32} = \frac{\bar{n}}{a}$$

where $k = \pi/L$ and $\bar{n} = n/a$.

APPENDIX B

The differential operators, stiffness, geometrical stiffness and mass matrices of classical theory are defined in this Appendix.

$[L_c]$ *operator*

$$L_{c11}() = A_{11}()_{,xx} + \frac{2A_{16}}{a}()_{,x\theta} + \frac{A_{66}}{a^2}()_{,\theta\theta}$$

$$L_{c12}() = L_{c21}() = \left(A_{16} + \frac{B_{16}}{a}\right)()_{,xx} + \frac{1}{a}\left(A_{12} + A_{66} + \frac{B_{12}+B_{66}}{a}\right)()_{,x\theta} + \frac{1}{a^2}\left(A_{26} + \frac{B_{26}}{a}\right)()_{,\theta\theta}$$

$$L_{c13}() = L_{c31}() = \frac{1}{a}\left(A_{12}()_{,x} + \frac{A_{26}}{a}()_{,\theta}\right) - B_{11}()_{,xxx} - \frac{3B_{16}}{a}()_{,xx\theta} - \frac{B_{12}+2B_{66}}{a^2}()_{,x\theta\theta} - \frac{B_{26}}{a^3}()_{,\theta\theta\theta}$$

$$L_{c22}() = \left(A_{66} + \frac{B_{66}}{a} + \frac{D_{66}}{a^2}\right)()_{,xx} + \frac{2}{a}\left(A_{26} + \frac{2B_{26}}{a} + \frac{D_{26}}{a^2}\right)()_{,x\theta} + \frac{1}{a^2}\left(A_{22} + \frac{2B_{22}}{a} + \frac{D_{22}}{a^2}\right)()_{,\theta\theta}$$

$$L_{c23}() = L_{c32}() = \frac{1}{a}\left(A_{26} + \frac{B_{26}}{a}\right)()_{,x} + \frac{1}{a^2}\left(A_{22} + \frac{B_{22}}{a}\right)()_{,\theta} - \left(B_{16} + \frac{D_{16}}{a}\right)()_{,xxx}$$
$$- \frac{1}{a}\left(B_{12} + 2B_{66} + \frac{D_{12}+2D_{66}}{a}\right)()_{,xx\theta} - \frac{3}{a^2}\left(B_{26} + \frac{D_{26}}{a}\right)()_{,x\theta\theta} - \frac{1}{a^3}\left(B_{22} + \frac{D_{22}}{a}\right)()_{,\theta\theta\theta}$$

$$L_{c33}() = \frac{A_{22}}{a^2}() - \frac{2}{a}\left(B_{12}()_{,xx} + \frac{2B_{26}}{a}()_{,x\theta} + \frac{B_{22}}{a^2}()_{,\theta\theta}\right) + D_{11}()_{,xxxx} + \frac{4D_{16}}{a}()_{,xxx\theta}$$
$$+ \frac{2D_{12}+4D_{66}}{a^2}()_{,xx\theta\theta} + \frac{4D_{26}}{a^3}()_{,x\theta\theta\theta} + \frac{D_{22}}{a^4}()_{,\theta\theta\theta\theta}.$$

$[L_{cg1}]$ *operator*

$$L_{cg1-11}() = L_{cg1-22}() = -L_{cg1-33}() = ()_{,xx}, \quad \text{all other } L_{cg1-ij}\text{s are zero.}$$

$[L_{cg2}]$ *operator*

$$L_{cg2-11}() = L_{cg2-22}() = L_{cg2-33}() = \frac{2}{a}()_{,x\theta}$$

$$L_{cg2-32}() = -L_{cg2-23}() = \frac{2}{a}()_{,x}, \quad \text{all other } L_{cg2-ij}\text{s are zero.}$$

$[L_{cg3}]$ *operator*

$$L_{cg3-11}() = L_{cg3-22}() = -L_{cg3-33}() = \frac{1}{a^2}()_{,\theta\theta}$$

$$L_{cg3-32}() = -L_{cg3-23}() = \frac{1}{a^2}()_{,\theta}$$